Clim. Past Discuss., 11, 4895–4915, 2015
www.clim-past-discuss.net/11/4895/2015/
doi:10.5194/cpd-11-4895-2015

Climate of the Past
Discussions

An astronomical correspondence to the 1470 year cycle of abrupt climate change

A. M. Kelsey[1], **F. W. Menk**[2], **and P. T. Moss**[1]

[1]School of Geography, Planning and Environmental Management, The University of Queensland, St Lucia, QLD, 4072, Australia
[2]Centre for Space Physics, School of Mathematical and Physical Sciences, Faculty of Science and Information Technology, University of Newcastle, Callaghan, NSW, 2308, Australia

Received: 9 September 2015 – Accepted: 22 September 2015 – Published: 20 October 2015

Correspondence to: A. M. Kelsey (alison.kelsey@uq.edu.au)

Published by Copernicus Publications on behalf of the European Geosciences Union.

Abstract

The existence of a ~1470 year cycle of abrupt climate change is well-established, manifesting in Bond ice-rafting debris (IRD) events, Dansgaard–Oeschger atmospheric temperature cycle, and cyclical climatic conditions precursory to increased El Niño/Southern Oscillation (ENSO) variability and intensity. This cycle is central to questions on Holocene climate stability and hence anthropogenic impacts on climate (deMenocal et al., 2000). To date no causal mechanism has been identified, although solar forcing has been previously suggested. Here we show that interacting combination of astronomical variables related to Earth's orbit may be causally related to this cycle and several associated key isotopic spectral signals. The ~1470 year climate cycle may thus be regarded as a high frequency extension of the Milankovitch precessional cycle, incorporating orbital, solar and lunar forcing through interaction with the tropical and anomalistic years and Earth's rotation.

1 Introduction

Rapid, millennial-scale climatic oscillations of 1470 ± 500 years are evident in numerous palaeoclimatic records in the North Atlantic and Pacific (Bond et al., 1997, 2013; Braun et al., 2005; Schulz, 2002; Turney et al., 2004). Greenland ice cores and North Atlantic marine cores show that abrupt climate change is associated with Dansgaard–Oeschger temperature cycles and IRD events (Bond et al., 1997; Bond and Lotti, 1995; Bond et al., 2013; Heinrich, 1988). Bond (Bond et al., 1997, 2013; Mayewski et al., 1997) demonstrated that millennial-scale climatic variability, operating continuously during the last glaciation and linked to atmospheric circulation disturbances over Greenland, continued into the Holocene as weakened IRD events in the North Atlantic. This cycle's periodicity of ~1470 ± 500 years is stable, and appears to be harmonically linked with the ~6100 year cycle associated with Heinrich IRD events during the last

CPD
11, 4895–4915, 2015

glacial, coincident with cold phases of the Dansgaard–Oeschger cycle (Bond et al., 1997; Mayewski et al., 1997; Schulz, 2002).

As sea-surface temperature (SST) cooling preceded these IRD events, and calving events occurred in multiple ice-sheets, internal factors to ice-sheet collapse were dismissed as causal (Bond et al., 1997; Bond and Lotti, 1995). Instead, an ocean–atmosphere link through solar forcing has been suggested (Bond et al., 1997; Mayewski et al., 1997; Schulz, 2002). It was hypothesised that the discharge of ice associated with IRD events produced colder, less saline waters, affecting the thermohaline current (THC), triggering abrupt major climate change (Clement and Peterson, 2008).

Correlated with Bond IRD and Dansgaard–Oeschger cycles is the 1480 ± 10 year cycle in the Pacific associated with the onset of climatic conditions suitable for increased El Niño/Southern Oscillation (ENSO) variability (Turney et al., 2004). ENSO's dynamic atmospheric–oceanic activity was proposed as an alternative cause of the millennial-scale climate cycle because associated convective systems dominate the planet's climate (Clement and Peterson, 2008). These systems witness the meridional poleward flow of heat, air and moisture from the tropics which is propelled by ocean–atmosphere interaction (Clement and Peterson, 2008; Gagan et al., 2004; Turney et al., 2004), and are hypothesised as contributing to ice surge and sea-ice formation through transported moisture and heat in the ~ 1470 year cycle (Gagan et al., 2004; Turney et al., 2004). Solar forcing of ENSO at orbital scales is evident in climatic datasets based on the relative precessional positions of the equinox and perihelion (Gagan et al., 2004; Turney et al., 2004).

Based on the similarity in lengths of this millennial-scale climate cycle and the Sothic cycle of Egyptian chronology (cf. Lockyer, 1964), we hypothesised that precession and rotation are contributing factors to the cause of the climate cycle. It was expected that, taken into consideration along with solar forcing, the cause of the ~ 1470 yr climate cycle could be explained. Such a conceptual model is important as the development of a conceptual framework that can contribute to the understanding radiocarbon vari-

CPD
11, 4895–4915, 2015

ability and long-term bolometric variability has been identified in understanding various isotopic signatures associated with this cycle (cf. Damon and Sonett, 1991).

2 Background

Variables were selected for this study to capture the elements of our conceptual model. As the Sun and Moon are responsible for the precessional cycle (Lowrie, 2007: 58), they were clear candidates. The Moon is responsible for nutation (Lowrie, 2007: 58). Nutation, which is a cyclical wobbling of the Earth's axis over a 18.6 yr periodicity, alters the latitudinal perspective to incoming solar radiation (Lowrie, 2007: 58). As Milankovitch demonstrated through his radiation curves that the amount of radiation received is latitudinally dependent (Imbrie and Imbrie, 1979), the selection of these variables was appropriate. Latitudinal variations in tide heights occur due to the lunar influence, also incorporating one of the conceptual model's precepts (cf. Lowrie, 2007: 52).

Solar forcing, through sunspot cyclicity and by association with the perihelion, was also incorporated in our model parameters. Sunspot activity modulates the cosmic ray flux in Earth's atmosphere (Libby, 1960), whilst the perihelion plays an important role in the level of solar insolation reaching Earth. Earth's rotation-revolution cycle relative to the anomalistic year, based on the perihelion, was also parameterised for this model. These combined factors were expected to account for the sub-harmonics of this millennial-scale signal and various other harmonics found in the radiocarbon isotopic record.

This conceptual model and its implementation are different from previous attempts to explain the cause of this ~ 1470 yr cycle. Firstly, an innovative approach used in this study is the inclusion of Earth's rotation relative to the anomalistic year in the search for a cause of this millennial-scale cycle and associated sub-harmonics. Unlike prior research into this subject, the novel use of astronomical data of solar and lunar declinations complements the simple trigonometric modelling used in our research.

CPD
11, 4895–4915, 2015

Whilst the Saros cycle of eclipses and lunar nodal cyclicity have been extensively used in prior research (Keeling and Whorf, 2000; Munk and Cartwright, 1966), we used the Metonic cycle of lunations within which a cyclical eclipse pattern is naturally self-contained (see below).

The Metonic lunation cycle recurs at 19 yr intervals (to within a couple of hours) and is therefore closely coupled to the tropical year. The Metonic return associated with the current perihelion was selected as a variable because it has the capacity to capture diachronic precessional dynamics by association with the anomalistic year: the Metonic cycle is naturally associated with the tropical system; and the length of the sidereal year is very close the anomalistic year. The Metonic cycle also fulfils the eclipse and gravitational potential of the vacant lunar nodal position as the Moon aligns with the nodes. Additionally, the Metonic cycle shares a harmonic with the Schwabe sunspot cycle at 57 yrs, enhancing its suitability for use in this model. Consequently, the Metonic cycle is an ideal variable that can be associated with both solar and lunar forcing, and is commensurate with the other variables unlike the Saros cycle of eclipses (cf. Cartwright, 1974; Munk et al., 2002).

The Saros cycle and nodal return are problematic for a number of reasons; these include the irregularities associated with the Saros cycle of eclipses (Keeling and Whorf, 2000), and the appropriateness of using the Saros cycle (Munk et al., 2002). The Saros cycle is one that has been known since ancient times, enabling the prediction of the occurrence of eclipses that recur in the same part of the heavens every 18 yrs 11 days (Gutzwiller, 1998: 596). Keeling and Whorf (2000) used the Saros cycle in their modelling attempt to explain the cause of the 1470 yr cycle but encountered difficulties that resulted in disparities between peaks of their interacting variables and tidal peaks, as well as large time discrepancies. Their (Keeling and Whorf, 2000) selection of incommensurate variables was problematic relative to the perigee's relationships with both the Saros cycle and perihelion (Cartwright, 1974; Munk et al., 2002). Additionally, because the relationship between the tropical solar cycle and Saros cycle produces a basic harmonic of ~ 1800 yrs, it is not suitable for investigating the cause of the ~ 1470 yr

CPD
11, 4895–4915, 2015

cycle because it is larger than the cycle being investigated. Keeling and Whorf (2000) generalised their connection to the ∼ 1470 yr cycle through a lunar forced ∼ 1800 yr cycle, but were not able to explain the mechanisms behind the variations or time discrepancies. The gravitational forcing mechanism used by Keeling and Whorf (2000), which influenced the vertical mixing of oceanic layers, was not seen as of great enough magnitude to cause the ∼ 1470 yr cycle (Munk et al., 2002).

Additionally, the use of lunar nodal cycle of ∼ 18.6 yrs as a variable is also inappropriate because it needs to be coupled with a lunation to fulfil its potential. This explains past interest in the Saros cycle of eclipses (Keeling and Whorf, 2000; Munk et al., 2002; Pettersson, 1930). The lunar nodes are the intersections of the ecliptic and lunar orbital plane, and are points at which solar and lunar eclipses occur when the Moon is within ∼ 11° of the node, at which time an eclipse must occur (Lowrie, 2007: 58). Exact alignments of the Moon and node result in total solar and lunar eclipses, as well as annular solar eclipses. The closer the Moon to these nodes, the greater the gravitational pull on Earth as individual gravitational influences align (cf. Lowrie, 2007: 50–59; Pettersson, 1930: 282–283). The Metonic cycle of lunations is a far more suitable for the purposes of investigating lunar-forced climate cycles.

3 The Model

This study presents a simple trigonometric model involving the superposition of mean values of three variables: (i) Schwabe sunspot cycle; (ii) Metonic cycle of lunations associated with the current perihelion, and (iii) the anomalistic year, the time for Earth's passage from perihelion to perihelion (365.2596 days). This in turn determines the time of Earth's rotation and revolution (RRA) relative to the perihelion, i.e. the time for perihelion to occur over the same geographic longitude on Earth. The RRA periodicity used was ∼ 103.77 years, which is the first closest rotational return to within 1° of the starting geographic longitude. This RRA variable is found in the radiocarbon spectral frequencies (Damon and Sonett, 1991; Sonett and Suess, 1984; Stuiver and Braziu-

CPD
11, 4895–4915, 2015

An astronomical correspondence to the 1470 year cycle of abrupt climate change

A. M. Kelsey et al.

nas, 1989), and the 209 year Suess de Vries (SdV) cycle is a harmonic of this cycle. The modelled RRA activity was compared to 5500 years of astronomical data based on solar and lunar declinations linked to the current perihelion-based Metonic lunation [Fig. 1], generated using planetarium software: NOVA 2.13, (Hand, 1989–1994) and SkyChart III (DeBenedictis, 1993–2004). Lunar nodal positions were also examined relative to these positions.

Heinrich (1988) suggested solar modulation of the climate as a factor in his model but qualified that it would need to accommodate locational sensitivity to filter the stronger pulses of ice-rafting. Our conceptual model assumes geographic regions that are sensitive to astronomical forcing through periodic orientation to peak solar and lunar influences (via rotation and revolution), with geographic longitude delineating cyclic returns. These sensitive regions occupy key locations associated with ENSO phenomena, IRD events, deep-water formation (DWF) and upwelling within the THC, with the inferred ability to influence atmospheric and oceanic circulation, heat distribution, and moisture transport. Such areas include the West Pacific Warm Pool (Partin et al., 2007) and areas of DWF in the North Atlantic (Bond et al., 2013; Clement and Peterson, 2008) and Weddell and Ross Seas (Mueller et al., 2012; Pritchard et al., 2012).

4 Discussion

Solar forcing and lunar forcing have both been suggested individually as causes of the ~ 1470 yr cycle of abrupt climate change, with schools of thought divided into two primary opposing camps (Broecker, 2003; Munk et al., 2002). Insolation vs. gravitation are the respective themes of these two hypothetical positions (Munk et al., 2002). Gravitational forcing is closely linked with theories connected to the thermohaline current and IRD events, whilst the argument for insolation is strongly linked with millennial-scale oscillations of ENSO in the tropical Pacific (Broecker, 2003). However, the position adopted in our conceptual model is one of joint gravitational-insolation influences as the cause of this cycle.

CPD
11, 4895–4915, 2015

The Sun and Moon cause oceanic, atmospheric and gravitational tides on Earth, driving wind and ocean currents (Keeling and Whorf, 2000; Lowrie, 2007; Toggweiler and Russell, 2008; Wilson, 2013), and their combined influence is potentially significant in the cause of the ~ 1470 yr climate cycle, given that linked atmospheric–oceanic coupling has been identified as a major driver of climate change (deMenocal et al., 2000). Both lunar tidal patterns (Oost et al., 1993; Pettersson, 1930; Raspopov et al., 2011; Stuiver et al., 1995) and evidence of solar forcing (Bond et al., 1997; Heinrich, 1988; Turney et al., 2004; Turney and Palmer, 2007) are found in the palaeoclimatic record.

The 11.4 year sunspot cycle appears to be associated with short-term signals and harmonics in palaeoclimatic radioisotopes datasets, as well as temperature cyclicity (Damon and Sonett, 1991; Eddy, 1976). These cosmogenic isotopes likely result from solar modulation of the interplanetary magnetic field and associated cosmic ray flux reaching Earth, and are anticorrelated with sunspot count (Stuiver and Braziunas, 1989; Stuiver and Quay, 1980). Medium-term cyclical wiggles of 209 yrs in the radiocarbon isotope curve, known as the SdV cycle, are assumed to be a modulation of cosmic ray flux by the solar wind (Damon and Sonett, 1991; Suess, 2006). On this assumption, modelling has suggested that the superposition of the ~ 209 year SdV and ~ 88 ± 11 year Gleissberg solar cycles may be associated with this ~ 1470 year climate cycle (Braun et al., 2005; Damon and Sonett, 1991). However, with only ~ 200 years of reliable direct observations of sunspot activity (Damon and Sonett, 1991; Eddy, 1976; Stuiver and Quay, 1980), solar variability for medium to long-term cycles is inferred from these isotopic datasets (Damon and Sonett, 1991).

The perihelion is a time of maximum annual solar insolation and an annual peak in spring tide (Berger, 1991; Lowrie, 2007; Thomson, 1997) and its timing is influenced by the Moon. The perihelion is nonstationary, moving in an open-ended cycle of ~ 110 ky (based on the length of the anomalistic year) and is an integral component of the Milankovitch precessional cycle (~ 21 ky) (Berger, 1977a, 1977b; Lowrie, 2007: 59). This precessional signal is evident in palaeoclimatic records and has been associated

CPD
11, 4895–4915, 2015

with IRD events, Dansgaard–Oeschger oscillations, and ENSO variability (Bond et al., 1997; Heinrich, 1988; Turney et al., 2004). The Milankovitch precessional cycle results from the interaction of two nonstationary precessional cycles that move in opposite directions: apsidal (perihelion/aphelion) and equinoctial precessions (Berger, 1977a; Imbrie and Imbrie, 1979). The equinoctial precession sees the equinoxes, which occur at the intersections of the celestial equator with the ecliptic, move in retrograde motion through the constellations over ~26 ky (Berger, 1977a). This movement is in opposite direction to the apparent annual solar path through the constellations.

The modelled cyclicity of Earth's RRA is similar to known isotopic spectral peaks in palaeoclimatic records (Bond et al., 1997; Damon and Sonett, 1991; Stuiver and Braziunas, 1989), with the strongest of such signals associated with RRA returns to the same longitude ($\leq 1.54°$) phase-aligned to the sunspot and perihelion-based Metonic cycles. As seen in Table 1, the shortest RRA cycle associated with a Metonic return is 493 years ($< 0.2°$), and these returns occur in conjunction with a series of Metonic eclipses (Fig. 1). Crosses in the right hand columns of Table 1 identify the coincidence of sunspot and Metonic cycles with the RRA cycle, which are important in the amplification of their individual influences. The 1479 year ($< 0.6°$) cycle (Table 1) is a harmonic of this signal, amplifying the phase-aligned sunspot cycle; it is also the mean length of the climate signal during the early Glacial (Bond et al., 2013). The RRA cycle period is also similar (differs by 104 years) to the mean Holocene length at 1375 years (Bond et al., 2013).

The Metonic lunation and Schwabe sunspot cycles are harmonically related at periods of 57 and 114 years, representing potential peaks/troughs of gravitational influence and temperature, with gravitational stresses greatest during solar eclipses. These periods appear in palaeoclimatic records (Chambers et al., 2012; Edvardsson et al., 2011; Stuiver and Braziunas, 1989). The 57 year cycle is nonstationary, returning to its starting longitude after 285 years (Table 1; Fig. 2).

Interestingly, the 209 year Suess de Vries and ~2300 year Hallstadt (Damon and Sonett, 1991) cycles are produced by the interacting variables of this model; the SdV

CPD
11, 4895–4915, 2015

cycle (Fig. 3a) matches the RRA return to ∼ 1.54° longitude of the start point, and the 1479 year cycle is within 0.59° (Table 1). The RRA-Metonic return (209 years), based on interaction between the Moon and Earth's rotation, is closer to the SdV cycle than it is to the return based on interaction between the sunspot cycle and Earth's rotation (RRA) (∼ 206 years) (Fig. 3b). These findings suggest that both the SdV and Hallstadt cycles result from the superposition of solar and lunar forcing.

The cycle with the most precise return to the starting longitude is 1868 years (0.017°) and has no correspondence to the sunspot and Metonic cycles, but appears as a major spectral signal in palaeoclimatic data (Bond et al., 2013). This cycle appears to be strongly associated with oceanic tidal forcing, coincident with the Moon at perigee and lunar node at 1842 yrs (Keeling and Whorf, 2000); at 1842 yrs a Metonic return occurs in association with a neap tide at the starting geographic longitude as the RRA is 90° out of alignment (< 0.18°). A 133 yr radiocarbon spectral signal (Damon and Sonett, 1991) is also reflected in the astronomical data of solar declinations (Fig. 1); it and the sunspot cycle are factors of the ∼ 1470 yr cycle.

From our astronomical data, sinusoidal curves representing lunar and solar declinations (Fig. 1) correspond with key isotopic spectral frequencies in palaeoclimatic datasets, including the 209 year and 228 year harmonics (lunar declinations) and a 133 year Metonic harmonic (solar declinations). A series of total and annular solar eclipses occurs as part of the Metonic-perihelion lunation series at ∼ 456 ± 38 yr intervals, as the lunar nodal axis aligns with the semi-major axis of Earth's orbit and hence the apsidal axis (Fig. 1). Bond IRD events occurred close to this harmonic at ∼ 1470 ± 500 year intervals (Fig. 1), suggesting a causal relationship with both the RRA and Metonic-perihelion cycles. The Little Ice Age (LIA) produced the latest Bond IRD event (Bond et al., 2013) closely associated with Metonic-perihelion eclipses, coincident with a total south nodal eclipse.

These Metonic eclipses (Fig. 1) were only total when the Moon was at the south lunar node. As total eclipses can only occur when the Moon is at perigee, this Metonic series of eclipses (Fig. 1) naturally subsumes the perigean cycle. Consequently, enhanced

CPD
11, 4895–4915, 2015

gravitational forces associated with the lunar perigee cycle are also captured by this model and reflected in associated astronomical data. Three out of four Bond cycles in the last 5000 yrs (Fig. 1) occurred in close proximity to these south nodal total eclipses in the Metonic eclipse series. These results support the hypothesis of the perigean cycle being involved in the cause of the 1470 yr cycle (cf. Keeling and Whorf, 2000; contra Munk et al., 2002).

These Metonic total and annual solar eclipses were ushered in and out by partial solar eclipses. Each eclipse series includes 4–5 solar eclipses spanning a period of 57–76 yrs. The 76 yr cycle has been associated with the Gleissberg cycle by some sources (eg., Hunten et al., 1993). Given that at 57 yr intervals the sunspot harmonic phase aligns with the Metonic cycle, phase-alignment of solar and lunar forcing can be theoretically demonstrated. These cycles were phase-aligned in 1954 when a sunspot minimum occurred (Nicholson, 1956) in conjunction with a perihelion-based Metonic eclipse (Table 2), after which sunspot numbers rose rapidly during Solar Cycle 19 (Nicholson, 1956). This eclipse occurred at midday at 145° E geographical longitude, which transverses the IPWP.

Previously, latitudinally dependent Milankovitch radiation curves demonstrated that astronomical cycles cyclically influence insolation based on orientation and solar proximity (Imbrie and Imbrie, 1979). Consequently, variations in data of solar and lunar declinations that are considered in this model are indicative of altered isotopic patterns of incoming solar radiation found in isotopic datasets. Furthermore, the 57 year Metonic-sunspot cyclicity appears to correspond to nonstationary 57 year patterns of precipitation, SST, sea level peaks, and geomagnetic cycles (Chambers et al., 2012; Edvardsson et al., 2011; Stuiver and Quay, 1980).

Our modelling and astronomical data suggest that a ∼ 493 year cycle is the base harmonic of ∼ 1470 yr cycle of climate change, resulting from the amplification of the Metonic-RRA cycle (493 yrs) by phase alignment with the sunspot cycle at ∼ 1480 yrs. The RRA's 493 year harmonic is proximate to the Metonic cycle harmonic of 494 years, phase-aligning with the 1482 year Metonic-sunspot harmonic at 1479 years. Based on the 493 yr cycle, at ~ 2300 years a phase shift occurs to realign the RRA cycle to within a 1° return to the starting geographical longitude, highlighting regional sensitivity.

Based on modelling of the 493 year cycle, there are generally three to four RRA series running concurrently that are within 1° of a longitudinal return, with a new series beginning every 1868 years. This period matches the most precise RRA return that can also be associated with an ~ 1800 year oceanic tidal cycle and major spectral peak in IRD data (Bond et al., 1997). Trough to peak of each series is a maximum of 2465 years that may be associated with the Hallstadt cycle. The maximum length of each series is 4437–4930 years that may be associated with the occurrence of Heinrich events.

5 Conclusions

By the RRA mechanism, the North Atlantic's IRD and Dansgaard–Oeschger cycles are phase-locked to internal climate events and to millennial-scale climatic variability of ENSO phenomena. The confluence of solar insolation extremes and peak gravitational, oceanic, and atmospheric tides at the same longitudes likely affects ice-sheet mechanics, oceanic and atmospheric currents, and atmospheric temperatures and SST, influencing ice-rafting events and freshwater discharge into areas of DWF of the THC (Clement and Peterson, 2008; de Juan et al., 2010; Mueller et al., 2012; Pritchard et al., 2012), as well as ENSO's dynamic atmospheric–oceanic activity.

In conclusion, we have seen that the superposition of the Earth's rotation cycle (RRA), perihelion-based Metonic cycle, and Schwabe sunspot cycle emulate the ~ 1470 climate cycle and its harmonics. Wobbles in solar and lunar declinations associated with this model match spectral frequencies in isotopic data and suggest that nutation affects Earth's insolation at sub-Milankovitch frequencies, influencing climate and isotopic patterns; although previously the cause of these isotopic patterns has been interpreted as inferred medium- to long-term cycles of solar variability (Damon and Sonett, 1991). The physical mechanisms for doing so are gravitational and radiative forcing inducing responses in Earth's internal climatic system.

CPD
11, 4895–4915, 2015

Acknowledgements. We thank the School of Geography, Planning and Environmental Management at the University of Queensland for research funding.

References

Berger, A.: Long-term variations of the Earth's orbital elements, Celestial Mech., 15, 53–74, 1977a.

Berger, A. L.: Support for the astronomical theory of climatic change, Nature, 269, 44–45, 1977b.

Berger, A.: Long-term history of climate ice ages and Milankovitch periodicity, in: The Sun in Time, Sonett, C. G., M., Matthews, M. (Eds.), University of Arizona, Tucson, 1991.

Bond, G., Showers, W., Cheseby, M., Lotti, R., Almasi, P., deMenocal, P., Priore, P., Cullen, H., Hajdas, I., and Bonani, G.: A pervasive millennial-scale cycle in north atlantic holocene and glacial climates, Science, 278, 1257–1266, 1997.

Bond, G. C. and Lotti, R.: Iceberg discharges into the North Atlantic on millennial time scales during the last glaciation, Science, 267, 1005–1010, 1995.

Bond, G. C., Showers, W., Elliot, M., Evans, M., Lotti, R., Hajdas, I., Bonani, G., and Johnson, S.: The north atlantic's 1–2 kyr climate rhythm: relation to Heinrich events, Dansgaard/Oeschger cycles and the little ice age, in: Mechanisms of Global Climate Change at Millennial Time Scales, American Geophysical Union, 2013.

Braun, H., Christl, M., Rahmstorf, S., Ganopolski, A., Mangini, A., Kubatzki, C., Roth, K., and Kromer, B.: Possible solar origin of the 1470 year glacial climate cycle demonstrated in a coupled model, Nature, 438, 208–211, 2005.

Broecker, W. S.: Does the trigger for abrupt climate change reside in the ocean or in the atmosphere?, Science, 300, 1519–1522, 2003.

Cartwright, D. E.: Years of peak astronomical tides, Nature, 248, 656–657, 1974.

Chambers, D. P., Merrifield, M. A., and Nerem, R. S.: Is there a 60 year oscillation in global mean sea level?, Geophys. Res. Lett., 39, 1–6, 2012.

Clement, A. C. and Peterson, L. C.: Mechanisms of abrupt climate change of the last glacial period, Rev. Geophys., 46, RG4002, doi:10.1029/2006RG000204 , 2008.

Damon, P. and Sonett, C.: Solar and atmospheric components of the atmospheric 14C variation spectrum, in: The Sun in Time, Sonett, C., Giampapa, M., and Matthews, M. (Eds.), University of Arizona, Tucson, 1991.

DeBenedictis, T.: SkyChart II I, Southern Stars Group, San Francisco, C A., 1993–2004.

de Juan, J., Elósegui, P., Nettles, M., Larsen, T. B., Davis, J. L., Hamilton, G. S., Stearns, L. A., Andersen, M. L., Ekström, G., Ahlstrøm, A. P., Stenseng, L., Khan, S. A., and Forsberg, R.: Sudden increase in tidal response linked to calving and acceleration at a large Greenland outlet glacier, Geophys. Res. Lett., 37, doi:10.1029/2010GL043289, 2010.

deMenocal, P., Ortiz, J., Guilderson, T., and Sarnthein, M.: Coherent high- and low-latitude climate variability during the Holocene warm period, Science, 288, 2198–2202, 2000.

Eddy, J. A.: The Maunder Minimum, Science, 192, 1189–1202, 1976.

Edvardsson, J., Linderholm, H. W., and Hammarlund, D.: Enigmatic cycles detected in subfossil and modern bog-pine chronologies from southern Sweden, Trace, 9, 173–180, 2011.

Gagan, M. K., Hendy, E. J., Haberle, S. G., and Hantoro, W. S.: Post-glacial evolution of the Indo-Pacific Warm Pool and El Niño–Southern oscillation, Quatern. Int., 118–119, 127–143, 2004.

Gutzwiller, M. C.: Moon-Earth-Sun: the oldest three-body problem, Rev. Mod. Phys., 70, 589–639, 1998.

Hand, R.: NOVA 2.13, Astrolabe Inc., Brewster, MA, 1989–1994.

Heinrich, H.: Origin and consequences of cyclic ice rafting in the Northeast Atlantic Ocean during the past 130,000 years, Quaternary Res., 29, 142–152, 1988.

Hunten, D. M., Gerard, J.-C., and Francois, L. M.: The atmosphere's response to solar radiation, in: The Sun in Time, Sonett, C., Giampapa, M., and Matthews, M. (Eds.), Generic, Kalmbach Publishing Company, Milwaukee, 1993.

Imbrie, I. and Imbrie, K.: Ice Ages: solving the Mystery, Enslow Publishers, New Jersey, 1979.

Keeling, C. D. and Whorf, T. P.: The 1800-year oceanic tidal cycle: a possible cause of rapid climate change, P. Natl. Acad. Sci. USA., 97, 3814–3819, 2000.

Libby, W. F.: Radiocarbon Dating, http://www.nobelprize.org/nobel_prizes/chemistry/laureates/1960/libby-lecture.pdf, last access: 23 October 2012, 2012.

Lockyer, S. N.: The Dawn of Astronomy, The MIT Press., Cambridge, 1964.

Lowrie, W.: Fundamentals of Geophysics, Cambridge University Press, Cambridge, 2007.

Mayewski, P. A., Meeker, L. D., Twickler, M. S., Whitlow, S., Yang, Q., Lyons, W. B., and Prentice, M.: Major features and forcing of high-latitude Northern Hemisphere atmospheric cir-

CPD
11, 4895–4915, 2015

culation using a 110,000-year-long glaciochemical series, J. Geophys. Res.-Oceans, 102, 26345–26366, 1997.
Mueller, R. D., Padman, L., Dinniman, M. S., Erofeeva, S. Y., Fricker, H. A., and King, M. A.: Impact of tide-topography interactions on basal melting of Larsen C Ice Shelf, Antarctica, J. Geophys. Res., 117, doi:10.1029/2011JC007263, 2012.
Munk, W., Dzieciuch, M., and Jayne, S.: Millennial climate variability: is there a tidal connection?, J. Climate, 15, 370–385, 2002.
Munk, W. H. and Cartwright, D. E.: Tidal spectroscopy and prediction, Philos. Tr. R. Soc. S.-A., 259, 533–581, 1966.
Nicholson, S. B.: Solar activity in 1955, Publ. Astron. Soc. Pac., 68, 146–148, 1956.
Oost, A. P., de Haas, H., Ijnsen, F., van den Boogert, J. M., and de Boer, P. L.: The 18.6 yr nodal cycle and its impact on tidal sedimentation, Sediment. Geol., 87, 1–11, 1993.
Partin, J. W., Cobb, K. M., Adkins, J. F., Clark, B., and Fernandez, D. P.: Millennial-scale trends in west Pacific warm pool hydrology since the Last Glacial Maximum, Nature, 449, 452–455, 2007.
Pettersson, O.: The Tidal Force, Geogr. Ann., 12, 261–322, 1930.
Pritchard, H. D., Ligtenberg, S. R. M., Fricker, H. A., Vaughan, D. G., Broeke, M. R. v. d., and Padman, L.: Antarctic ice-sheet loss driven by basal melting of ice shelves, Nature, 484, 502–505, 2012.
Raspopov, O. M., Dergachev, V. A., Ogurtsov, M. G., Kolström, T., Jungner, H., and Dmitriev, P. B.: Variations in climate parameters at time intervals from hundreds to tens of millions of years in the past and its relation to solar activity, J. Atmos. Sol.-Terr. Phy., 73, 388–399, 2011.
Schulz, M.: On the 1470 year pacing of Dansgaard–Oeschger warm events, Paleoceanography, 17, 1014, doi:10.1029/2000PA000571, 2002.
Sonett, C. P. and Suess, H. E.: Correlation of bristlecone pine ring widths with atmospheric 14C variations: a climate–sun relation, Nature, 307, 141–143, 1984.
Stuiver, M. and Quay, P. D.: Changes in atmospheric carbon-14 attributed to a variable sun, Science, 207, 11–19, 1980.
Stuiver, M. and Braziunas, T. F.: Atmospheric 14C and century-scale solar oscillations, Nature, 338, 405–408, 1989.

CPD
11, 4895–4915, 2015

An astronomical correspondence to the 1470 year cycle of abrupt climate change

A. M. Kelsey et al.

Stuiver, M., Grootes, P. M., and Braziunas, T. F.: The GISP2 δ18O climate record of the past 16,500 years and the role of the sun, ocean, and volcanoes, Quaternary Res., 44, 341–354, 1995.

Thomson, D. J.: Dependence of global temperatures on atmospheric CO2 and solar irradiance, P. Natl. Acad. Sci. USA, 94, 8370–8377, 1997.

Toggweiler, J. R. and Russell, J.: Ocean circulation in a warming climate, Nature, 451, 286–288, 2008.

Turney, C. S. M. and Palmer, J. G.: Does the El Niño–Southern Oscillation control the inter-hemispheric radiocarbon offset?, Quaternary Res., 67, 174–180, 2007.

Turney, C. S. M., Kershaw, A. P., Clemens, S. C., Branch, N., Moss, P. T., and Keith Fifield, L.: Millennial and orbital variations of El Nino/Southern Oscillation and high-latitude climate in the last glacial period, Nature, 428, 306–310, 2004.

Wilson, I. R. G.: Long-term lunar atmospheric tides in the southern hemisphere, The Open Atmospheric Science Journal, 7, 51–76, doi:10.2174/1874282320130415001, 2013.

Table 1. RRA returns (< 2°) to the same geographical longitude. Note the presence of important spectral signals, including the Suess de Vries cycle and variations of the ~ 1470 yr cycle.

Period (yrs)	Cycle Return (°)	Precision(°)	Phase Alignment Sunspot	Metonic	(yrs)
0	0	0			
1868	0.017	0.017			
1375	359.82	0.18			
493	0.197	0.197		x	494
2361	0.215	0.215	x		2360
882	359.623	0.377			
986	0.395	0.395		x	988
2257	359.443	0.557	x		2257
389	359.425	0.575	x		388
1479	0.592	0.592	x	x	1482
1764	359.245	0.755			
104	0.772	0.772	x		103
1972	0.789	0.789	x		1972
1271	359.048	0.952			
597	0.969	0.969			
2465	0.986	0.986			
778	358.851	1.149			
1090	1.166	1.166			
285	358.654	1.346	x	x	285
1583	1.364	1.363			
2153	358.608	1.392			
1660	358.472	1.526			
208	1.544	1.542	x	x	209
2076	1.561	1.561	x		2075
1167	358.276	1.724			
701	1.741	1.741			
2542	358.096	1.904			
674	358.079	1.921	x		673
1194	1.938	1.938			

CPD
11, 4895–4915, 2015

Table 2. Perihelion-based Metonic eclipses (1916–2011). Details of these eclipses show eclipse/lunation date, nodal type, and lunar and solar declinations and right ascension (R.A.). Data generated by Skychart III and NOVA 2.13.

Year	Date	Lunation type	Node type	Solar declination	Solar R.A.	Lunar declination	Lunar R.A.
2011	4 Jan	Partial eclipse	North	−22.73	284.82	−21.75	284.72
1992	4 Jan	Annular eclipse	North	−22.72	285.05	−22.35	285.00
1973	4 Jan	Annular eclipse	North	−22.68	285.38	−22.93	285.40
1954	5 Jan	Annular eclipse	North	−22.68	285.43	−23.58	285.55
1935	5 Jan	Partial eclipse	North	−22.72	285.15	−24.27	285.33
1916	5 Jan	Lunation		−22.77	284.70	−24.95	284.93

CPD
11, 4895–4915, 2015

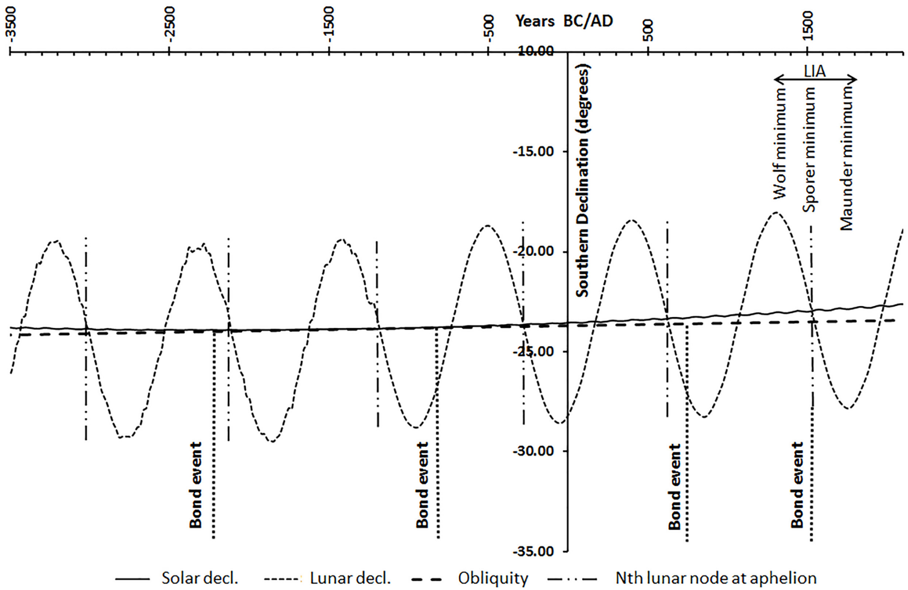

Figure 1. Solar and lunar declination interaction of the Metonic-perihelion cycle at 19 yr intervals. Bond IRD events occurred close to the lunar nodes at aphelion/perihelion. Total and annular solar eclipses occur at the juncture of these solar and lunar declinations. The relationship of these cycles to the ecliptic is shown through the dotted line associated with obliquity. Solar declinations form the solid sinusoidal curve, and lunar declinations the dashed sinusoidal curve; the dashed line is the ecliptic.

CPD
11, 4895–4915, 2015

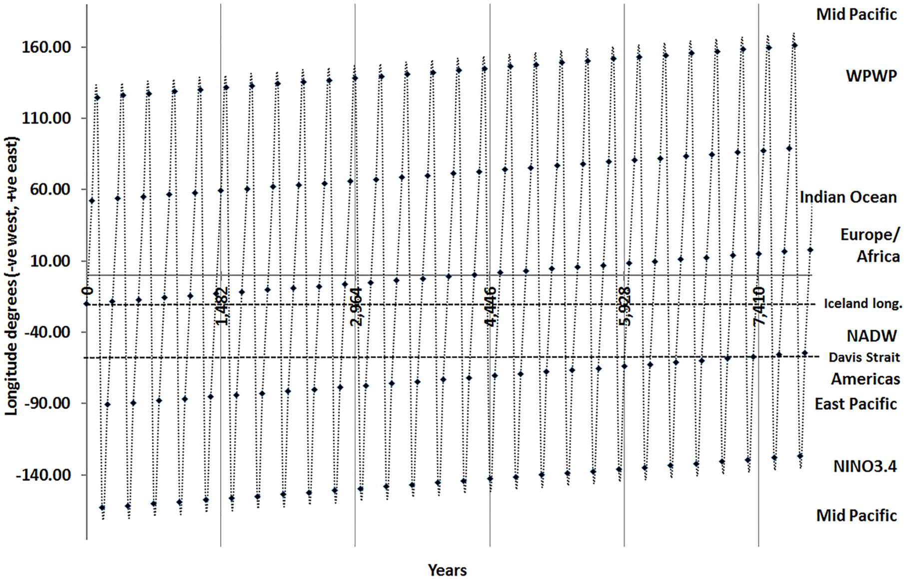

Figure 2. The 57 year Metonic-sunspot cycle in geographic context. Vertical axis represents geographic longitude and horizontal axis time in years, from an arbitrary start for 80 centuries. Time between points on the Metonic-sunspot curve is 57 years, and time between points at the same longitude is 285 years. The 1482 year Metonic-sunspot period (solid vertical lines) is close to the RRA cycle of 1479 years. The 285 year and 1482 year periodicities are harmonics of the 57 year cycle.

CPD
11, 4895–4915, 2015

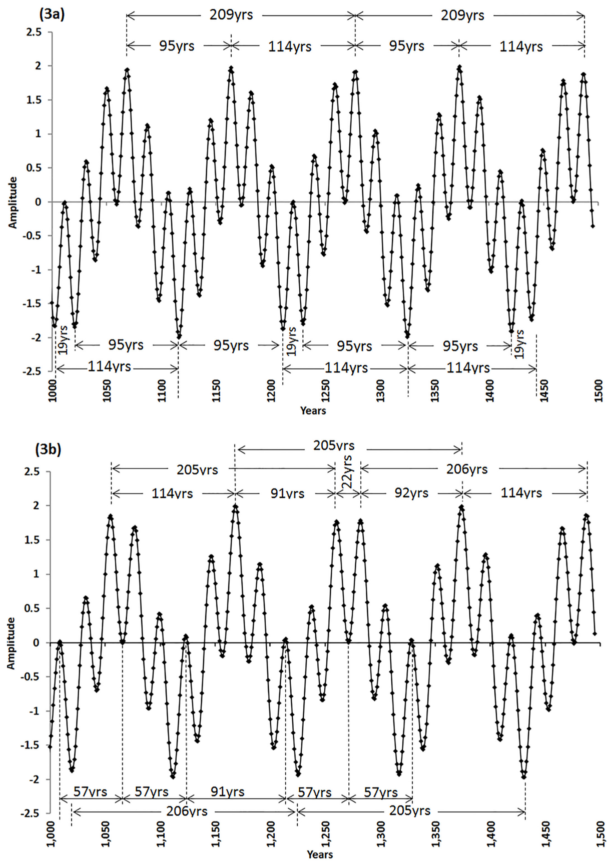

Figure 3. SdV and Gleissberg cycles. Combination of the RRA, Metonic and sunspot cycles reproduce the SdV and Gleissberg cycles; **(a)** Combined RRA and Metonic sinusoidal curves SdV (209 years) and Gleissberg (95 years); **(b)** Combined RRA and sunspot sinusoidal curves: SdV (205–206 years) and Gleissberg (91 years).